The Astrophysical Journal, 665:L39–L42, 2007 August 10

FAR-ULTRAVIOLET OBSERVATIONS OF THE LOOP I/NORTH POLAR SPUR REGION

J.-W. Park,[1] K.-W. Min,[1] K.-I. Seon,[2,3] I.-J. Kim,[1] Y.-M. Lim,[1] W. Han,[2] U.-W. Nam,[2]
J.-H. Park,[2] J. Edelstein,[3] E. J. Korpela,[3] and R. Sankrit[3]
Received 2007 April 18; accepted 2007 June 21; published 2007 July 26

ABSTRACT

The results of diffuse far-ultraviolet observations of the Loop I/North Polar Spur (NPS) region are presented in this Letter. Several important ionic emission lines, including C IV, Si II*, Si IV, and Al II, were detected. Fluorescent emission lines from hydrogen molecules were also seen in the spectra. A spectral image made with C IV emission shows a shell-like feature colocated with the X-ray NPS. This feature is located just inside the Loop I radio ridges. Another interesting C IV feature is seen at the inner edge of the "interaction ring," where the cold interstellar medium is in direct contact with the X-ray–bright hot gas. The present observation is in good agreement with a model of recent supernova explosion in an inhomogeneous medium, possibly disturbed by previous multiple supernova explosions.

Subject headings: ISM: bubbles — ISM: individual (Loop I, North Polar Spur) — supernova remnants — ultraviolet: ISM

1. INTRODUCTION

The Loop I/North Polar Spur (NPS) region was initially identified as the ridges of an enhanced continuum emission in radio wavelengths near the northern Galactic pole (Quigley & Haslam 1965). Subsequent observations revealed its proximity to the solar system with a distance of ~120 pc (Bingham 1967). It was also shown to have a large angular size of ~116° (Berkhuijsen et al. 1971).

The region was soon found to emit enhanced soft X-rays (Bunner et al. 1972). *ROSAT* observations later revealed that the NPS region was filled with a hot gas, with a prominent feature shown to be located inside Loop I ridges in a 0.75 keV soft X-ray image (Snowden et al. 1995). The origin of the hot gas was initially attributed to a single supernova explosion (Cruddace et al. 1976). Soon, however, other scenarios were suggested that were quickly deemed more plausible for this huge object. For example, Iwan (1980) proposed that a second supernova remnant shock adjacent to the NPS, such as Loop IV, may be responsible for the bright X-rays associated with the NPS. Egger (1995) argued that the object could be a superbubble filled with a shock-heated gas produced by stellar winds or successive supernova explosions in the Scorpio-Centaurus (Sco-Cen) OB association, which is located ~170 pc from the solar system and is located inside the Loop I. In this scenario, the asymmetric appearance of Loop I was attributed to an off-center explosion of the most recent supernova approximately 2×10^5 yr ago (Egger 1995).

Egger & Aschenbach (1995) also noted the possibility of a collision of a Loop I superbubble with the Local Bubble (LB), a cavity filled with hot tenuous plasma of $T \sim 10^6$ K that surrounds the solar system (Cox & Reynolds 1987). They argued that the dense toroidal shell seen in the radio image, which is coincident with a region of low X-ray emission well inside Loop I, is the interaction zone ("interaction ring") of the two superbubbles. Recently, high-resolution hydrodynamic simulations have been carried out for the interaction of Loop I and the LB in a realistically evolving ambient medium (Breitschwerdt & Avillez 2006). According to the model, Loop I and the LB were generated in the inhomogeneous background interstellar medium, disturbed already by multiple supernova explosions for 200 Myr. Their result not only reproduces observed features such as the interaction ring of the two superbubbles but also gives the O VI column density for the LB in excellent agreement with observations, with the age of the LB constrained to be ~14.5 Myr.

Hence, the Loop I/NPS region is an interesting object where a hot gas interacts with a cool and dense H I interstellar medium. This provides a good opportunity for the study of the evolution of a superbubble or supernova remnant. The results of far-ultraviolet (FUV) observations of this object made with the Spectroscopy of Plasma Evolution from Astrophysical Radiation (SPEAR), also known as the Far-Ultraviolet Imaging Spectrograph (FIMS) are reported in this Letter. Several important ionic emission lines, including C IV and Si II*, were detected, and spectral images for these two lines were constructed.

2. OBSERVATIONS AND DATA REDUCTION

SPEAR/FIMS is a dual-channel FUV imaging spectrograph ("Short" wavelength channel [S] 900–1150 Å, "Long" channel [L] 1330–1720 Å; $\lambda/\Delta\lambda \sim 550$) with a large field of view (S channel: 4.0° × 4.6′, L channel: 7.5° × 4.3′) and an imaging resolution of 5′–10′ along the slit. It is designed to observe diffuse FUV emission lines. SPEAR/FIMS was launched on 2003 September 27 on the Korean microsatellite *STSAT-1*. Additional information concerning the instrument, mission, and data analysis procedures are given in Edelstein et al. (2006a, 2006b). As the main purpose of the present Letter is to construct spectral images for the C IV and Si II* emission lines, only the L channel data was analyzed.

The present analysis of the Loop I region was based on the 430 orbits of sky-survey data made between March 12 and July 8 of 2004. As Loop I occupies a vast region close to the north Galactic pole, nearly 25% of all observations in sky-survey mode passed through this giant target when sweeps were made along constant ecliptic longitudes from the north ecliptic pole to the south ecliptic pole through the antisolar point. The analysis was limited to the halo region including NPS above the Galactic latitude $b = 25°$ and bounded by the Galactic

[1] Korea Advanced Institute of Science and Technology (KAIST), 373-1 Guseong-dong, Yuseong-gu, Daejeon 305-701, South Korea; yharock9@space.kaist.ac.kr.
[2] Korea Astronomy and Space Science Institute (KASI), 61-1 Hwaam-dong, Yuseong-gu, Daejeon 305-348, South Korea.
[3] Space Sciences Laboratory, University of California, Berkeley, 7 Gauss Way, Berkeley, CA 94720.

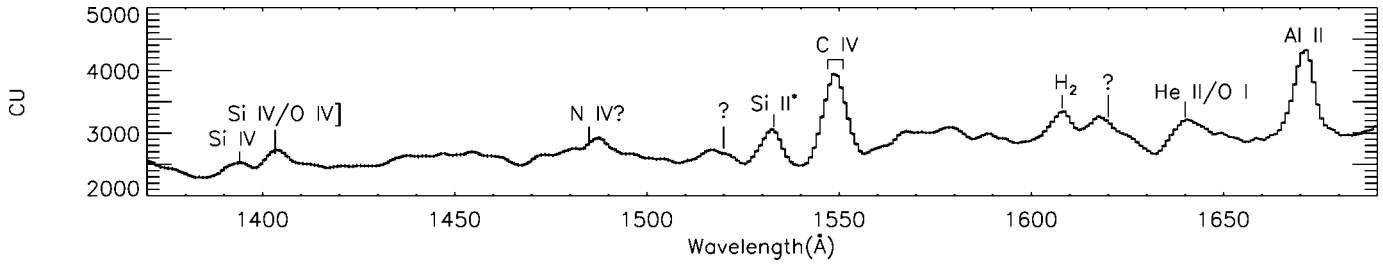

FIG. 1.—Spectrum of the entire region selected for this study. The original spectrum was binned with a width of 1 Å and smoothed with a Gaussian smoothing scale of 1 Å. The error bars range from 12 to 29 CU (continuum intensity units, photons cm^{-2} s^{-1} sr^{-1} $Å^{-1}$), which are small compared to the observed intensities.

longitudes $l = -90°$ and $+90°$, although Loop I extends to the southern hemisphere. The halo region is less contaminated than the low-latitude region by emissions from bright stars, which are difficult to separate from diffuse emissions. Additionally, the bright X-ray region below $b = 25°$ has been associated with the Galactic bulge (see, e.g., Sanders et al. 1993). The total exposure time for the selected region was $\sim 5.3 \times 10^4$ s, and the average exposure time for each pixel was 9.4 s with a maximum of 48.4 s.

Data reduction was carried out as follows: First, to avoid contamination from bright O and B stars, events observed with a count rate higher than 1000 counts s^{-1}, which represents nearly 13 times the median count rate for this region, were removed. This procedure removed ~7.3% of the total photon events. The photon and exposure events were then binned using the equal-area Hammer-Aitoff projection in Galactic coordinates, and a three-dimensional count rate array (l, b, λ) with $1.^\circ2 \times 1.^\circ2$ spatial bins and 1 Å wavelength bins was created. A spectral image was obtained by taking a portion of the spectral data around the emission line of interest from each pixel and fitting this with a constant continuum plus a Gaussian function. Spectral resolution at the given line was employed as the width (FWHM) of the Gaussian function. The final image was constructed using the method of adaptive smoothing to increase the signal-to-noise ratio (S/N; Seon et al. 2006). The Gaussian smoothing scale varied from 1.2° to 6°.

3. ANALYSIS AND RESULTS

Figure 1 shows the L channel spectrum for the entire region selected in this study, smoothed with a Gaussian function whose width (FWHM) is 1 Å. Removed from the original spectrum was the short-wavelength region below 1370 Å as well as the long-wavelength region above 1690 Å, which were contaminated by the O I airglow line at 1356 Å and a relatively large detector background at long wavelengths, respectively. What remains of the spectrum shows clearly several ionic emission lines, including Si II* λ1533 and C IV λλ1548, 1551 emission lines. A companion of Si II at 1527 Å is not seen, most likely due to resonant scattering as Si II λ1527 is the transition to the true ground state and is likely to be optically thick in a warm ionized medium (WIM; Korpela et al. 2006). The prominent peak at 1671 Å is attributed to Al II. The wiggles near 1400 Å appear to be O IV] multiplets blended with a Si IV doublet. The peak at 1640 Å may corresponds to He II and the O I airglow. The emission line at 1608 Å is identified as a fluorescent emission from molecular hydrogen.

In Figure 2, the results of the L channel continuum map (1370–1690 Å) and the spectral images made with the C IV and Si II* emission lines are shown, as is the Hα map. The C IV image was constructed by fitting the spectral data in the 1532–1568 Å range from each pixel with two Gaussian profiles centered at 1548 and 1551 Å, respectively, with the line ratio $\lambda 1548 : \lambda 1551 = 2 : 1$. The Si II* line was fitted for the spectral range of 1528–1548 Å with a single Gaussian profile centered at 1533 Å. The high-intensity features in these spectral images, especially those shown in blue, are all with S/N > 3, while some of the features in yellow with intensity <2000 LU (line intensity units, photons cm^{-2} s^{-1} sr^{-1}) have S/N < 2. The Hα map was adapted from Finkbeiner (2003). Also shown in Figure 3 are images seen in 0.75 keV X-rays, 0.25 keV X-rays, 21 cm H I emission, and 100 μm infrared, for comparison. These maps were adapted from the archival data of the SkyView

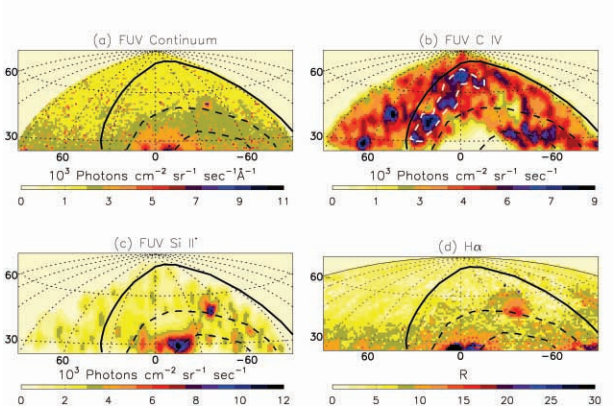

FIG. 2.—SPEAR/FIMS spectral images of Loop I/NPS and the ambient halo region together with the Hα map. The solid curve and the two dashed curves represent the radio Loop I and the interaction ring, respectively (Egger & Aschenbach 1995). (*a*) SPEAR/FIMS continuum map; (*b*) SPEAR/FIMS C IV map; (*c*) SPEAR/FIMS Si II* map; (*d*) Hα map (Finkbeiner 2003). The C IV NPS is marked by a dashed white line in (*b*).

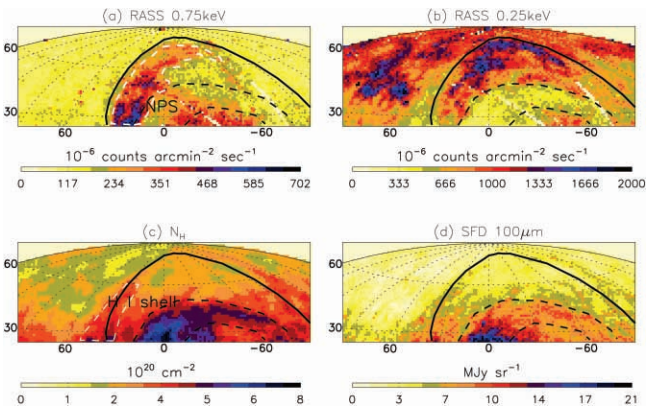

FIG. 3.—Images of the same region shown in Fig. 2 in other wavelengths, adapted from the archival data of the SkyView Observatory (McGlynn et al. 1998). (*a*) RASS 0.75 keV map (Snowden et al. 1995); (*b*) RASS 0.25 keV map (Snowden et al. 1995); (*c*) N_H map (Dickey & Lockman 1990); (*d*) SFD 100 μm map (Schlegel et al. 1998). The X-ray NPS and H I shell are marked by dashed white lines in both (*a*) and (*c*), respectively.

Observatory (McGlynn et al. 1998); they are, respectively, from the 0.75 and 0.25 keV *ROSAT* All-Sky Survey (RASS) maps (Snowden et al. 1995), the Dickey & Lockman maps (Dickey & Lockman 1990), and the Schlegel-Finkbeiner-Davis (SFD) maps (Schlegel et al. 1998). In these figures, the radio continuum of Loop I is indicated by a solid line, and the boundaries of the interaction ring by two dashed lines, inside of which is a region with $N(\mathrm{H\,I}) > 7 \times 10^{20}$ cm^{-2}, in accordance with the definition of Egger & Aschenbach (1995).

As shown in Figure 2*a*, the intensity of the FUV continuum increases gradually toward the lower Galactic latitude and peaks at the center. A similar trend is also seen in the Hα map of Figure 2*d*, while the dust map of Figure 3*d* more strongly resembles the continuum map, implying that the FUV continuum in the present case is primarily due to the scattering of starlight by dust. The bright spot near (l, b) = (315°, +50°) in Figure 2*a* corresponds to the H II region ionized by the nearby (88 pc) B-type star Spica (Reynolds 2004). It is seen that the same region is bright in Hα, while there is no counterpart in the dust map.

The C IV map of Figure 2*b* shows a well-defined high-intensity region close to Loop I (*a solid curve*), whose boundary is indicated by a dashed white line. This "C IV NPS" is colocated with the X-ray NPS seen in the 0.75 keV map shown in Figure 3*a*. The C IV NPS looks disconnected in the middle (l = 15°, b = +45°) because of the low S/N there. Another interesting C IV enhancement is seen near the inner edge of the interaction ring, at the interface between the high-density H I tail of the interaction ring (Fig. 3*c*) and the region of the enhanced 0.75 keV X-ray below the interaction ring (Fig. 3*a*). Also observable are a couple of local patches of enhanced C IV emissions outside Loop I, in the vicinity of bright 0.25 keV X-ray regions. These patches have no counterparts in the 0.75 keV X-ray map. In effect, aside from the bright patches, the general background intensity of C IV outside Loop I is essentially identical to that inside Loop I, as in the 0.25 keV X-ray map, while the 0.75 keV X-ray map shows marked enhancement only inside Loop I. In addition, it is notable that the central region at lower Galactic latitudes is void of C IV emissions, as in the 0.25 keV X-ray map, whereas this region is filled with H I and dust.

The Si II* map in Figure 2*c* is very different from that of the C IV. First, it should be noted that the C IV or X-ray–bright NPS region is not bright in Si II*. Instead, bright patches of Si II* are more prevalent around the interaction ring in the western part of Loop I. Second, Si II* is most bright in the H II region of Spica and in the central region of low Galactic latitudes where dust is thick. These results are not untenable, as Si II* is known to trace a WIM ($T \sim 10^4$ K) such as an H II region, while silicon is also believed to condense to form dust grains.

4. DISCUSSION

It is shown in Figures 2*b* and 2*c* that C IV and Si II* enhancement is widespread over the entire region selected for the present study, as in the case of the 0.25 keV X-ray, which is believed to come from the LB, a Galactic halo, and a combination of solar charge exchange (Bellm & Vaillancourt 2005). Previous observations of C IV and O VI have revealed a prevalent but irregular distribution of these highly ionized species in the halo region (Martin & Bowyer 1990; Savage et al. 2003). In the present C IV map, it was found that more than 60% of the pixels showed a positive detection of this ion with S/N > 3; less than 20% of them showed null detection. The average C IV intensity of the region outside Loop I was estimated to be 5384 ± 147 LU, which is comparable to the values obtained by Martin & Bowyer (1990) for a halo region that varied from 2200 to 5700 LU.

As shown in Figure 2*b*, the C IV NPS appears to be an incomplete shell similar to that seen in the 0.75 keV X-ray image. It is colocated at the X-ray NPS, a feature expected from the interaction of a supernova remnant with an ambient interstellar medium. Egger (1995) proposed that the radio Loop I shell can be explained by the stellar winds from the Sco-Cen association with a dynamical age of $\sim 2 \times 10^7$ yr. He also argued that the X-ray emission from the interior of the neutral shell may be attributed to a recent supernova event within the association through the tenuous medium in the radio Loop I shell; the resulting age of the remnant in this case is 2×10^5 yr. According to a simulation study by Shelton (1998, 1999) that is relevant to the evolution of a supernova remnant in a lower halo region, a cool shell develops behind the shock front at the end of an adiabatic phase, and a hot supernova bubble slowly radiates away what remains of its energy. Hence, the remnant appears to be strongly edge-brightened in the FUV emission from highly ionized species such as C IV, while the central region is filled with hot gas, which appears bright in X-rays. In the present case of Loop I, much of the X-ray emission from the central hot gas appears to be blocked by the interaction ring.

The intensity of the C IV NPS is estimated to be nearly 8000 LU, including the contribution from the diffuse component as the background or foreground, which is ~5400 LU. The remaining 2600 LU may come purely from the NPS. We note that the source inherent intensity before extinction could be even higher. These estimations are higher than the values obtained from the model study of Shelton (1998) in which 1600–940 LU is expected from the supernova remnant of the age between 1×10^5 and 2.5×10^5 yr. However, it should be noted that the surrounding medium of the NPS might have been denser than the value (0.01 cm^{-3}) modeled in the simulation, as it was close to the preexisting Loop I ridges. In fact, Egger (1995) showed that the density of the preexisting tenuous medium of $n_0 = 0.63$ cm^{-3} could explain the observed velocity of the H I shell of ~21 km s^{-1}.

The recent simulation study of Breitschwerdt & Avillez (2006) may provide a more realistic model for the region of Loop I and the LB. According to the simulation, the temperature of the Loop I shell is $\sim 10^{5.8}$ K at the present epoch, which yields the emission measure 0.75 cm^{-6} pc for the observed intensity of C IV NPS, assuming collisional ionization equilibrium (Mazzotta et al. 1998) and cosmic abundance. Further assuming the path length through the shell to be 150 pc along the line of sight (Breitschwerdt & Avillez 2006; Willingale et al. 2003), we estimate the shell density to be ~0.07 cm^{-3}. The result is comparable to the value of X-ray analysis, ~0.03 cm^{-3} (Willingale et al. 2003). We thus conclude that the C IV intensity from the NPS is in reasonable agreement with the model of a supernova remnant in an inhomogeneous interstellar medium, possibly disturbed by previous multiple supernova explosions.

Another interesting C IV emission feature is that at the inner edge of the tail section of the interaction ring in the western region of the low Galactic latitudes. This C IV enhancement may be due to thermal conduction or, more likely, turbulent mixing as the supernova-induced flows are highly turbulent (Breitschwerdt & Avillez 2006; Slavin et al. 1993). Patches of Si II* enhancement are also seen in the vicinity of the interaction ring in the western region. However, they seem to have originated from the foreground compared with the interaction ring, as background emissions are mostly blocked by the dense interaction

ring. These enhanced Si II* patches may originate from the low-temperature ($10^{3.5}$–$10^{3.9}$ K) local H I clouds detached from the interaction ring (Breitschwerdt et al. 2000). The two bright C IV patches in the eastern region of Loop I do not appear to be associated with the "H I shell" seen in Figures 3*c*. In contrast, Slavin (1989) calculated some of the strongest emission lines from local clouds and obtained 278 LU for C IV, which is much less than the observed intensity in the present study.

5. CONCLUSION

We have presented the results of FUV observations of the Loop I/NPS region, including the ambient halo region, with a total of 180° × 65° sky around the north Galactic pole. A C IV image confirmed that this region is filled with a hot gas, previously shown by X-ray observations. A shell-like C IV emission feature at the inner edge of Loop I, coincident with the hot X-ray region, shows cooling at the limb of a hot gas. This hot gas is generated by a supernova explosion in the preexisting inhomogeneous medium. It was also observed that the C IV emission is prominent at the boundary between the hot X-ray gas and the cool interaction ring, where turbulent mixing of the two gases is likely to occur. On the other hand, Si II* toward the interaction ring may arise from a local H I cloud, such as the local interstellar cloud.

SPEAR/FIMS is a joint project of KAIST, KASI, and the University of California, Berkeley (UCB). It is funded by the Korean Ministry of Science and Technology and by NASA grant NAG 5-5355. NASA's SkyView facility was utilized as part of this study (http://skyview.gsfc.nasa.gov). The authors appreciate the referee for helpful comments.

REFERENCES

Bellm, E. C., & Vaillancourt, J. E. 2005, ApJ, 622, 959
Berkhuijsen, E. M., Haslam, C. G. T., & Salter, C. J. 1971, A&A, 14, 252
Bingham, R. G. 1967, MNRAS, 137, 157
Breitschwerdt, D., & de Avillez, M. A. 2006, A&A, 452, L1
Breitschwerdt, D., Freyberg, M. J., & Egger, R. J. 2000, A&A, 361, 303
Bunner, A. N., Coleman, P. L., Kraushaar, W. L., & McCammon, D. 1972, ApJ, 172, L67
Cox, D. P., & Reynolds, R. J. 1987, ARA&A, 25, 303
Cruddace, R. G., Friedman, H., Fritz, G., & Shulman, S. 1976, ApJ, 207, 888
Dickey, J. M., & Lockman, F. J. 1990, ARA&A, 28, 215
Edelstein, J., et al. 2006a, ApJ, 644, L153
———. 2006b, ApJ, 644, L159
Egger, R. J., 1995 in ASP Conf. Ser. 80, The Physics of the Interstellar Medium and the Intergalactic Medium ed. A. Ferrara et al. (San Francisco: ASP), 45
Egger, R. J., & Aschenbach, B. 1995, A&A, 294, L25
Finkbeiner, D. P. 2003, ApJS, 146, 407
Iwan, D. 1980, ApJ, 239, 316
Korpela, E. J., et al. 2006, ApJ, 644, L163
Martin, C., & Bowyer, S. 1990, ApJ, 350, 242
Mazzotta, P., Mazzitelli, G., Colafrancesco, S., & Vittorio, N. 1998, A&AS, 133, 403
McGlynn, T., Scollick, K., & White, N. 1998, in IAU Symp. 179, New Horizons from Multi-Wavelength Sky Surveys, ed. B. J. McLean et al. (Dordrecht: Kluwer), 465
Quigley, M. J. S., & Haslam, C. G. T. 1965, Nature, 208, 741
Reynolds, R. J. 2004, Adv. Space Res., 34, 27
Sanders, W. T., et al. 1993, Proc. SPIE, 2006, 221
Savage, B. D., et al. 2003, ApJS, 146, 125
Schlegel, D. J., Finkbeiner, D. P., & Davis, M. 1998, ApJ, 500, 525
Seon, K.-I., et al. 2006, ApJ, 644, L175
Shelton, R. L. 1998, ApJ, 504, 785
———.1999, ApJ, 521, 217
Slavin, J. D. 1989, ApJ, 346, 718
Slavin, J. D., Shull, J. M., & Begelman, M. C. 1993, ApJ, 407, 83
Snowden, S. L., et al. 1995, ApJ, 454, 643
Willingale, R., Hands, A. D. P., Warwick, R. S., Snowden, S. L., & Burrows, D. N. 2003, MNRAS, 343, 995